JMEPEG (2007) 16:22–29
DOI: 10.1007/s11665-006-9003-1

1059-9495/$19.00

Laser Cutting of Kevlar and Mild Steel Composite Structure: End Product Quality Assessment

F. Al-Sulaiman, B.S. Yilbas, C. Karatas, O. Keles, I. Uslan, Y. Usta, M. Ahsan, and A. Bazoune

(Submitted January 19, 2006; in revised form April 6, 2006)

In the present study laser cutting of composite structure, consisting of Kevlar laminate at the top and mild steel sheet at the bottom, is considered. The end product quality is assessed using the thermal cutting standards. To compare the end product quality of composite structure cuts, Kevlar laminate and mild steel sheet are cut using the same cutting parameters. The kerf widths for Kevlar laminate and mild steel sheet cuts are predicted from the analytical formulation based on the lump parameter analysis. It is found that the end product quality of composite structure cuts is lower than that corresponding to Kevlar laminate and mild steel sheet cuts.

Keywords composite, cutting, Kevlar, laser, quality

1. Introduction

Laser cutting of sheet materials finds wide application in industry due to its precision of operation and low cost. In general, an assisting gas is used during the laser machining operation. In this case, assisting gas jet emerging from a nozzle impinges onto a surface of the workpiece. Depending on the process requirements, assisting gas can be inert or reactive such as oxygen, which provides some extra energy in the cutting section through higher temperature exothermic reactions. On the other hand, non-reactive assisting gasses, such as argon or helium, shield the cutting environment and prevent the cutting section from oxidation reactions during the process. Non-reactive assisting gas is used for the processing of plastic or wood while oxygen is used for metallic material processing. In some cases, the non-metallic materials become part of metallic components through chemical bonding. The laser cutting of composite structure requires fine tuning of laser cutting parameters. Consequently, laser cutting of such components with high quality end product becomes fruitful. Consequently, investigation into such laser cutting situation becomes necessary.

Considerable research studies were carried out to examine laser cutting processes and end product quality assessment. The striation formation and oxidation dynamics of laser cutting process were examined by Ivarson et al. (Ref 1). They indicated that the possible source for striation formation was a cyclic variation in oxidation reactions as well as viscosity change of molten metal in the cut kerf. The formation of heat affected zone during laser cutting of stainless steel was examined by Sheng and Joshi (Ref 2). They determined the heat-affected zone through temperature field and compared with the experimental data. High power intensity laser cutting of steel was carried out by Grum and Zuljan (Ref 3). They used a factorial analysis to establish statistical relations among the variables of the laser cutting parameters. Laser machining of ceramics was investigated by Roy and Modest (Ref 4). They indicated that the predictions of groove shape produced by a

F. Al-Sulaiman, B.S. Yilbas, M. Ahsan, and **A. Bazoune,** KFUPM, Dhahran, Saudi Arabia; and **C. Karatas,** Hacettepe University, Ankara, Turkey; and **O. Keles, I. Uslan** and **Y. Usta,** Gazi University, Ankara, Turkey. Contact e-mail: bsyilbas@kfupm.edu.sa

List of Symbols

A	energy coupling factor, < 1
C_p	specific heat at constant pressure (J/kgK)
d	kerf depth (m)
f	fraction of pressure drop in the kerf, < 1
k	thermal conductivity (W/mK)
l	length of the cut (m)
L_b	latent heat of evaporation (J/kg)
L_m	latent heat of melting (J/kg)
P_g	assisting gas pressure (Pa)
M_w	molecular mass of assisting gas (g/mol)
P_{ow}	power input in the workpiece (W)
P_{ow0}	power input at the workpiece surface (W)
T_m	melting temperature (K)
T_0	ambient temperature (room temperature) (K)
v	laser beam cutting speed (m/s)
$\bar{v}$	average velocity of dross (m/s)
w	laser beam waist diameter at workpiece surface (m)
w_i	molten layer outer diameter in the cutting section (m)
w_k	kerf width (m)
w_0	beam waist diameter at surface when focus setting is nominal (m)
α	thermal diffusivity (m^2/s)
β	fraction of evaporation contribution, < 1
δ	molten material thickness in the cutting section (m)
σ	the molecular diameter (Å)
η_g	assisting gas viscosity (Pa.s)
η_u	super heating factor in the melt front, < 1
ρ	density of workpiece material (kg/m^3)
ρ_g	density of assisting gas (kg/m^3)

laser beam agreed well with the experimental results. Laser cutting process and influence of oxygen on the end product quality were examined by Yilbas et al. (Ref 5). They showed that increasing oxygen gas pressure influenced significantly the end product quality due to enhancement of oxidation reactions. The dynamics of ripple formation and melt flow in laser beam cutting were examined by Schulz et al. (Ref 6). They indicated that the surface tension effect had negligible contributions at the cutting front, but might stand to become dominant at the lower edge of the cutting front where the molten material separated from the solid material. The model study on material removal mechanisms in laser cutting was considered by Quintero et al. (Ref 7). The thickness of the molten layer was predicted and material removal mechanisms were discussed.

Composite materials may exhibit low cutting quality due to delamination and fiber spalling when machined with conventional tools. However, cutting quality improves significantly when machined with a laser beam. Considerable research studies were carried out to examine laser cutting of composites. Laser and water jet cutting of composite sheet materials were investigated by Shanmugam et al. (Ref 8). They indicated that both cutting methods provided high surface and structural integrity of the substrate material after the cutting process. Laser cutting of fiber-reinforced composite and end product quality assessment were carried out by Cenna and Mathew (Ref 9). They indicated that laser was very sensitive to process disturbances, which required sophisticated process monitoring and control. Laser cutting of composites and evaluation of material properties were conducted by Chen and Cheng (Ref 10). They modeled the cutting process and the predictions of heat-affected zone agreed with the experimental results. Excimer laser cutting of polyester resins and model studies were carried out by Galantucci and Giusti (Ref 11). They indicated that the numerical simulations, compared with the experimental cuts, gave good results in terms of shape and depth of cut. Laser cutting of fiber-reinforced polyesters were examined by Tagliaferi et al. (Ref 12). They showed that the thermal properties of the fibers and matrix were the principle factors that affected the cutting performance. Laser cutting of Kevlar was examined by Doyle and Kokosa (Ref 13). They showed that number of toxic and cancer-producing compounds were identified in the smoke plume produced.

In the present study, laser cutting of composite structure consisting of Kevlar and steel is studied. Kevlar laminate is situated at the top of the steel sheet in association with the application of frictional elements such as clutches used in the power transmission line. A CO_2 laser was used to cut the composite structures. The end product quality is assessed using the international standards for thermal cutting. In order to compare the end product quality of the laser-cut composite structures, Kevlar laminates and steel sheets were also cut individually. The kerf widths measured are compared with the predictions of the analytical formulation, which is based on the lump parameter analysis.

2. Experimental

The laser used in the experiment is a CO_2 laser (LC-αIII-Amada) and delivering nominal output power of 2000 W at pulse width different frequencies. Nitrogen emerging from a conical nozzle and co-axially with the laser beam is used. A 127 mm focal lens with defocusing facilities is used to focus the laser beam. One of the laser parameters varied in the experiment is the duty cycle. The duty cycle indicates the ratio of on/off of the laser power. The higher number of duty means higher ratio of on compared to off, and therefore, it gives more output energy. The duty cycle 100% means continuous on, which is, continuous wave (CW) cutting as depicted in Fig. 1(a). The initial temperature of workpieces prior to cutting is 294 K. The length of the laser cuts is extended to 100 mm for each cutting condition to obtain fair assessment for the cutting quality. The cutting conditions are given in Table 1.

The workpiece used in the experiment consists of Kevlar laminate and steel (DIN EN 10149, used as a metallic plate for

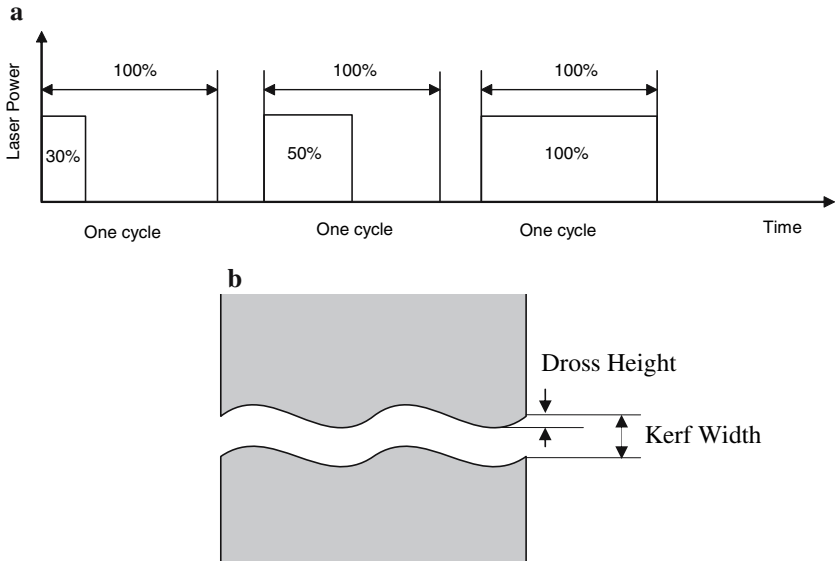

Fig. 1 (**a**) Duty cycle. (**b**) A schematic view of laser cut

Table 1 Laser cutting parameters

Feed, m/s	Power, kW	Duty Cycle	Frequency, Hz	Nozzle Gap, mm	Kevlar Thickness, mm	Steel Thickness, mm	Nozzle Diameter, mm	N_2 Pressure, kPa
0.67	1.5-2	0.35-1.0	300	1.5	0.5 & 0.8	1.2-3	1.5	600

Table 2 Elemental composition of steel used in the experiment

Fe	C	Si	Mn	P	S	Al	Nb	Ti	V
Balance	0.12	0.1	1.2	0.02	0.01	0.02	0.07	0.05	0.1

Table 3 Workpiece and assisting gas properties used in the simulations

Source of Variation	Value	Units
Density of assisting gas	2.0786	kg/m^3
Density of Kevlar	1340	kg/m^3
Fraction of evaporation contribution (β)	0.1	-
Fraction of pressure drop (*f*)	0.5	-
Energy coupling factor (*A*)	0.6	-
Super heating factor in the melt front (η_u)	0.01	-
Assisting gas pressure (P)	600	kPa
Molecular diameter of nitrogen	0.3176	Å
Heat of reaction of Kevlar	26.92×10^3	J/kg
Specific heat capacity of Kevlar	1400	J/kgK
Thermal conductivity of Kevlar	0.14	W/mK
Latent heat of fusion of steel	272,000	J/kg
Latent heat of evaporation of steel	6,258,154	J/kg
Specific heat capacity of steel	460	J/kgK
Thermal conductivity of steel	53	W/mK

a friction compound). Elemental composition of steel is given in Table 2. Kevlar laminate with 0.5 and 0.8 mm thicknesses is used, since it is the range of thickness being used as friction element in industry. The properties of Kevlar are given in Table 3.

SEM (JEOL JSM 6360LV) is used for micrographs of the cutting section while optical microscope is employed for kerf width size measurements.

3. Evaluation of Cut Quality

The cut quality may be evaluated in terms of dross height and out of flatness (Fig. 1b), at cut surface and the assessment for the cut quality is based on the international standards for thermal cuts (DIN2310). Height of dross was measured with a reading microscope in μm units.

4. Mathematical Analysis

When solid substrate is subjected to laser irradiation energy, energy balance among the absorbed laser energy, internal energy gain of the substrate material and losses due to convection and diffusion. The scaling law due to energy balance can yield the equation (Ref 14): In the analysis some useful assumptions are made. These include: constant physical properties are accommodated, the influence of surface plasma on heating situation is neglected, superheating in liquid phase and evaporation rates from the surface are considered to be small and presented as a fraction of latent heat of melting and evaporation, and assisting gas is considered to be an ideal gas. The energy balance at the laser irradiated surface yields the following relation (Ref 14):

$$\frac{P_{ow}}{d} = \frac{vw_k + A_3\sqrt{vw_k}}{A_0} \quad \text{(Eq 1)}$$

where P_{ow} is the laser output power and d is the spot diameter at the workpiece surface. A_0 and A_3 are:

$$A_0 = \frac{A}{a_0} \quad \text{and} \quad A_3 = \frac{1}{a_0}\frac{(w_k + 2w_k(T_m - T_0))}{2\sqrt{\alpha w w_k}} \quad \text{(Eq 2)}$$

and a_0 is:

$$a_0 = \rho\left(C_p(T_m - T_0) + L_m + \beta L_b\right) \quad \text{(Eq 3)}$$

where w_k is the kerf width, w the laser beam waist size, l the length of the cut, T_m the melting temperature of the substrate material, T_0 the ambient room temperature. β is the contribution of evaporation of the surface. It should be noted that during the laser cutting, most of the dross is removed from the cutting section by the assisting gas, provided that only a fraction of material vaporizes. Therefore, β takes the small value.

Laser-irradiated surface of the melt pool shape can be considered to be a semicircular ring of width δ, which is $\delta = \frac{(w_i - w_k)}{2}$, where w_i is the molten layer outer diameter and w_k is the kerf width. The mass balance in the kerf leads the following equation (Ref 14):

$$\frac{\delta}{d} = \frac{2v}{\pi v} \quad \text{(Eq 4)}$$

The momentum balance at assisting gas and melt interface enables to determine the average velocity of the melt. In this case, the drag force generated by assisting gas should be equal to the rate of momentum change of the melt. This leads to the following relation for the average velocity of the melt flow:

$$\bar{v} = \left[\frac{2\eta_g v_g d}{\pi\rho w_k \delta}\right]^{1/2} \quad \text{(Eq 5)}$$

where η_g and v are the viscosity and velocity of assisting gas, respectively.

Combining Eq (4) and (5) and introducing $\delta = \frac{(w_i - w_k)}{2}$ yield:

$$w_k = \frac{w}{1 + \left(\frac{4\rho v^2 d}{\pi\eta_g v_g}\right)} \quad \text{(Eq 6)}$$

Assisting gas pressure can be determined from:

$$v_g = \sqrt{\frac{2\Delta P_g}{\rho_g}} \quad \text{or} \quad v_g = \sqrt{\frac{2fP_g}{\rho_g}} \quad \text{(Eq 7)}$$

Moreover, the viscosity of assisting gas can be determined from ideal gas law approximation (Ref 15):

$$\eta_g = 2.927 \times 10^{-8} \frac{M_w}{\sigma^2} \sqrt{\frac{P_g}{\rho_g}} \quad \text{(Eq 8)}$$

where M and σ are molecular mass (g/mol) and molecular diameter (Å) of assisting gas, respectively. The units of η_g, P_g and ρ_g are Pa.s, Pa, and kg/m^3. To estimate the kerf width, the balance of heat flux at the maximum width of the liquid-solid interface can be used (Ref 16). This leads the following expression:

$$w_i = \sqrt{\frac{2\pi\alpha}{l}} \frac{A\eta_u(l+w)}{k(T_m - T_0)w} \frac{P_{ow}}{\sqrt{v}} \quad \text{(Eq 9)}$$

where A is the effective absorptivity of the substrate material, α is the thermal diffusivity, η_u is the melt superheating factor, k is the thermal conductivity. Combining Eq (1), (6) and (9), the following is resulted (Ref 14):

$$w_k = \frac{1}{v}\left[\frac{2.51\sqrt{\frac{\alpha}{w}}\frac{(2A\eta_u)}{k(T_m - T_0)}P_{ow}\sqrt{v}}{1 + 3.08 \times 10^7 \left(\frac{A_0}{A_3\sqrt{f}}\right)\left(\frac{\rho\rho_g\sigma^2\alpha}{M_w P f \sqrt{w}}\right)P_{ow}\sqrt{v}}\right] \quad \text{(Eq 10)}$$

where f is the fraction of pressure drop in the kerf, σ the molecular diameter (Å), M_w the molecular weight (g/mol unit) of the assisting gas, P and ρ_g the pressure and density of the assisting gas, and η_u the superheating factor in the melted zone.

The kerf width size is determined from Eq (10) using Mathematica Software Package. The properties of the substrate material and the assisting gas are given in Table 3. It should be noted that the latent heat of melting is replaced with the heat of reaction, since the combustion is the major process for mass removal from the kerf during the cutting.

5. Results and Discussion

Laser cutting of composite structures consisting of Kevlar, which is situated at the top, and mild steel substrate at the bottom is considered. The kerf width and dross height are measured to assess the resulting cut quality and the study is extended to include the comparison of the experimental results with the predictions obtained from the previous formulation (Ref 14). The measurement of dross height is carried out using a reading optical microscopy; in which case, actual dross height is measured. Table 1 gives the cutting parameters while Table 3 gives the simulation conditions.

Figure 2 shows kerf width measured and predicted from the simulation results for Kevlar laminate and mild steel sheet. The data presented correspond to the individual cutting of Kevlar laminate and mild steel sheet for different duty cycles, i.e. kerf width is measured for Kevlar and mild steel cuts separately. The kerf width resulted due to mild steel is less than that corresponding to Kevlar. This can be associated with the porous structure of the Kevlar laminate. In this case, the assisting gas used is nitrogen, which prevents the oxidation reactions and minimizes the sideways burning. Kevlar laminate with porous structure may capture oxygen molecules in the voids during its production. During the cutting process, oxygen releases and causes high-temperature oxidation reactions enhancing the sideways burning. This enlarges the kerf width during the cutting process. In addition, low thermal conductivity of Kevlar (Table 3) limits the diffusional energy dissipation from the kerf site to the substrate material. Consequently, energy available in the cutting section becomes large, which in turn, enhances the mass removal rate from the cutting section, i.e. kerf width increases. Moreover, increasing duty cycle enhances the kerf width due to high energy content of the large duty cycles, i.e. high energy content in the pulse accelerates the mass removal rate, and hence improving the kerf width size. When comparing predictions with the experimental results, it can be observed that both data agree well, provided that some small discrepancies occur between the predictions and the experimental results. In this case, experimental data are slightly higher than the predictions, which are more pronounced for mild steel. This may be because of the assumptions made in the analysis and some experimental errors. In the case of mild steel, the kerf width size is smaller than that of Kevlar. This is mainly because of high mass density and thermal conductivity of mild steel. Therefore, radial conduction reduces the energy available in the cutting section, which lowers the kerf width size. Moreover, increasing workpiece thickness increases the kerf width size, provided that this increase is small.

Figure 3 shows variation of the kerf width with increased duty cycle for different thicknesses of composite structures. The

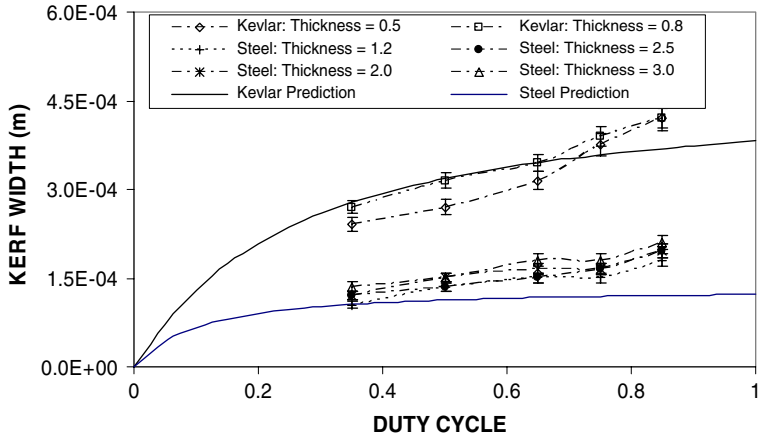

Fig. 2 Kerf width with duty cycle obtained from predictions and experiment for steel and Kevlar laminates

kerf width is measured for the combination of Kevlar and mild steel layered structure. The kerf width size increases significantly with increasing duty cycle as compared to Fig. 2. In addition, the magnitude of kerf width is higher than those shown in Fig. 2. This indicates that Kevlar laminate situated at the top surface of the mild steel modifies the cutting conditions significantly. In this case, the gas generated during the cutting of Kevlar has an adverse effect on the kerf size. In addition, it is possible that the focusing effect of the incident beam is modified by the Kevlar product created during the cutting process. This situation is more pronounced for the thick workpieces. In this case, the kerf width size increases almost 35% as the thickness of the mild steel sheet increases to 3 mm. This situation is elevated with increasing duty. Consequently, the probable distortion of the incident beam by Kevlar after cut-products results in excessive enlargement of the kerf width size.

Figure 4(a) shows the dross height with duty cycle for two Kevlar laminate thicknesses while Fig. 4(b) shows the dross

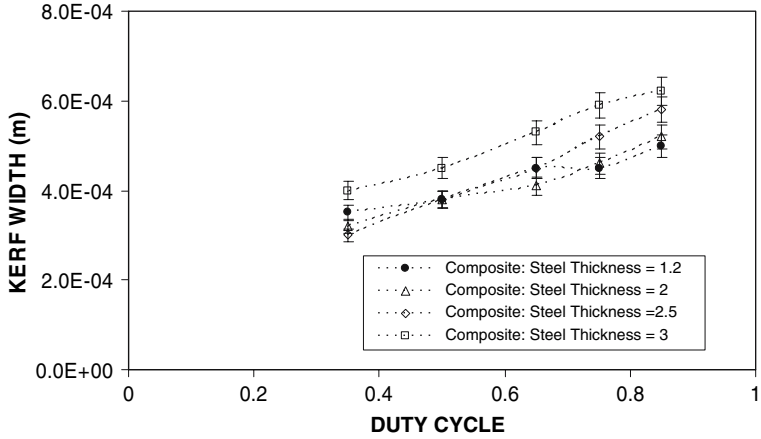

Fig. 3 Kerf width obtained from experiment for composite structure

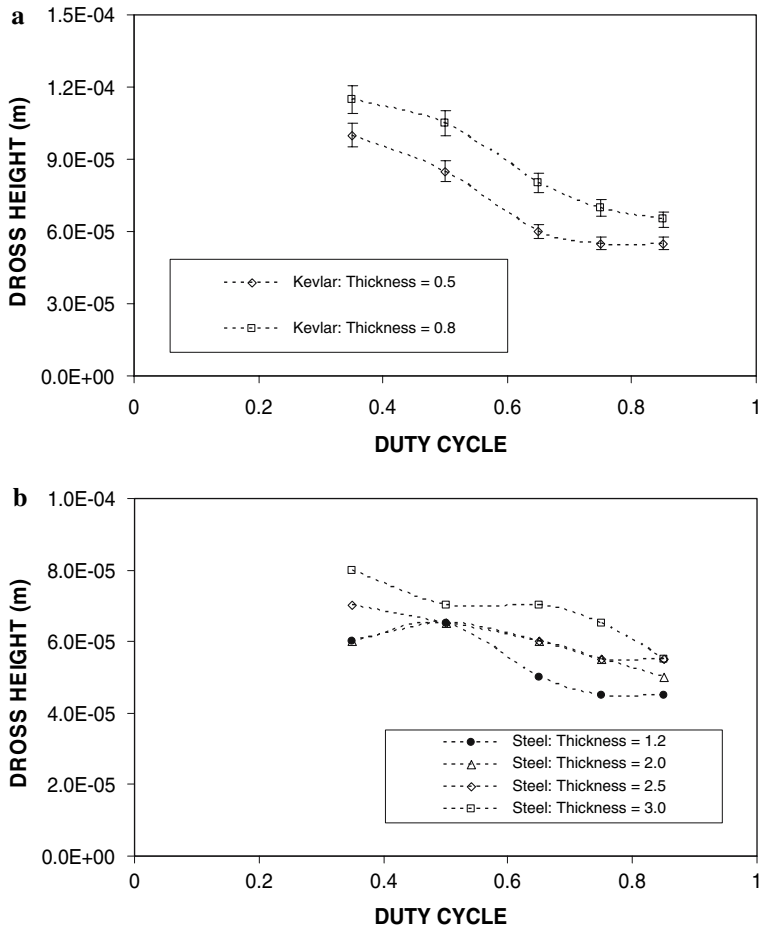

Fig. 4 (**a**) Dross height with duty cycle for Kevlar laminate. (**b**) Dross height with duty cycle for steel sheet

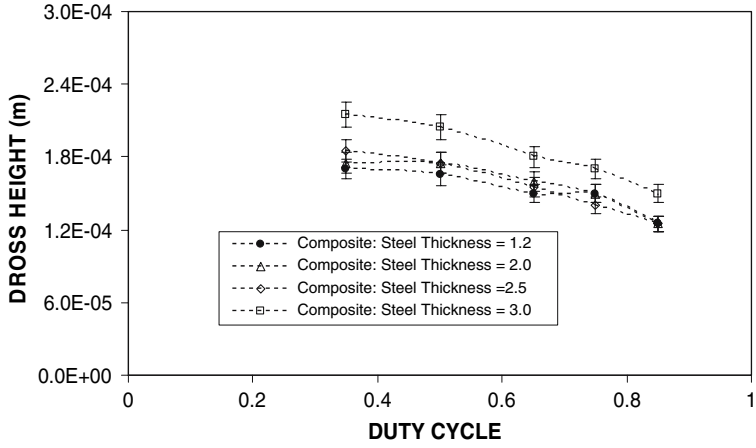

Fig. 5 Dross height with duty cycle for composite structure

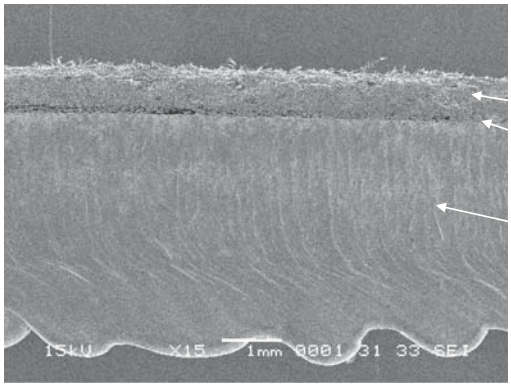

Attached Kevlar laminate on steel surface.

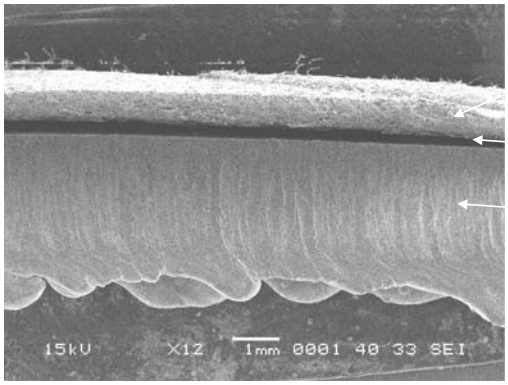

Detach Kevlar laminate from steel surface.

Fig. 6 Micrographs of composite structure cut sections

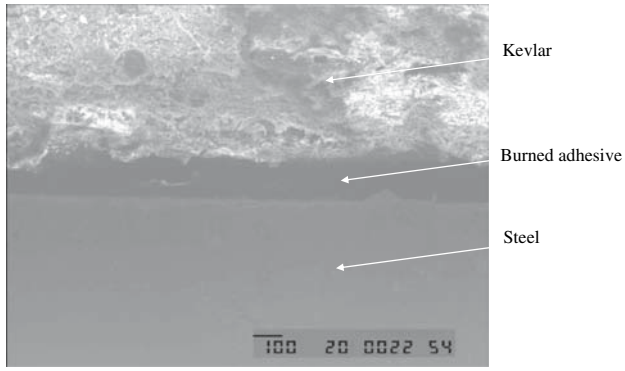

Fig. 7 Micrograph of cut section showing the interface of Kevlar and steel

height with duty cycle for four thicknesses of mild steel sheet. The dross height reduces with duty cycle for Kevlar and stainless steel workpieces. This indicates that cutting quality improves with increasing duty cycle. This, in turn, enhances the mass removal rate from the cut section. Moreover, the molten material ejected from the kerf site remains at high temperature due to incident high laser energy. This lowers the viscosity and the surface tension of the molten metal (Ref 5). Consequently, adherence of dross to the cut sections becomes minimal. Increasing the kerf width size due to high laser beam energy, increases the amount of molten material in the cut section. The moment of inertia of the molten metal, due to momentum exchange between the melt flow and the impinging gas, enhances. Therefore, the residence or attachment of the molten metal to the sides of the cut surfaces becomes minimal. This situation is more pronounced for mild steel workpieces due to high mass density, i.e. the dross height reduces significantly for mild steel workpieces.

Figure 5 shows dross height with duty cycle for the composite structure. The dross height corresponding to composite structure is considerably higher than those corresponding to Kevlar or steel cuts, provided that in all cases, the dross height reduces with increasing duty. High values of the dross height for composite structure show that cutting quality significantly reduces. This situation is true for all thicknesses of the mild steel sheets in composite structure. The possible explanation for the enhanced dross height is the distortion of the incident beam in the cutting section due to cutting product of Kevlar, which is placed on the top surface of the mild steel sheet. Consequently, laser cutting of composite structure, composing of two different properties of layers, does not result in reasonable good cutting quality.

Figure 6 shows micrographs of laser-cut edges of composite structure. The integrity of the Kevlar laminate and underneath mild steel is evident; however, separation of Kevlar laminate

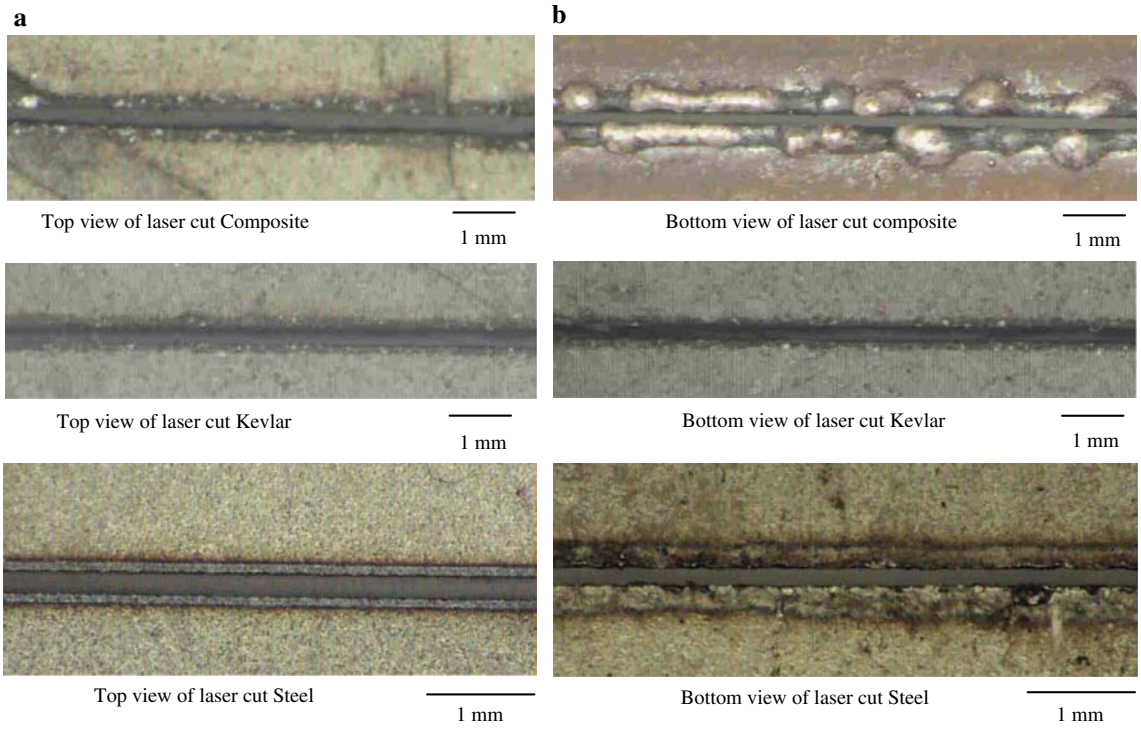

Fig. 8 (**a**) Photographs of top view of laser cut sections. (**b**) Photographs of bottom view of laser cut sections

from the mild steel surface also occurs in some cutting situations. The occurrence of laminate separation is because of the sideways burning of adhesive resin between the Kevlar laminate and mild steel surfaces. In this case, oxygen molecules captured in the Kevlar laminate close to mild steel surface triggers sideways burning of both Kevlar laminate and the resin. It should be noted that Kevlar laminate forms char for temperatures at around 620 K. Carbonization and charring of Kevlar surfaces next to the resin is observed after peeling off the laminate from mild steel surface. The micrograph of cut section with sideways burning of resin is shown in Fig. 7.

Figures 8(a) and 8(b) show optical photographs of top and bottom views of cuts corresponding to composite structure as well as Kevlar laminate and mild steel sheet. The globules formation around the cut edges at the rear side of the workpiece is evident for the composite structure. The formation of globules at cut edges lowers the cut quality significantly. The globules formation is due to attachment of the dross and molten metal to the cut edges because of high drag forces, i.e. drag force dominates the inertia force in the molten metal at the cut edges. In the case of Kevlar laminate and mild steel sheet cutting only, globules formation is minimal or non-existent. This clearly suggests that for quality processing, cutting of Kevlar laminate and mild steel sheets in required sizes separately and joining them together with resin becomes unavoidable due to the end product quality requirement.

6. Conclusions

Laser cutting of composite structure, consisting of Kevlar laminate at the top and mild steel sheet at the bottom, is considered. The cutting quality is assessed with international standards for thermal cutting. For comparison purpose, laser cutting of Kevlar laminates and mild steel sheets is also carried out. It is found that the kerf width size corresponding to composite structure is significantly higher than that of Kevlar laminates and mild steel sheets cuts. Enlargement of the size of the kerf width is more pronounced for high duty cycles. In this case, laser power intensity reaching the cutting section is modified by the Kevlar products formed during cutting process. The dross height for the composite structure is considerably higher than that corresponding to Kevlar laminate and mild steel sheets. This is more pronounced for low duty cycles. The micrographs of cut sections reveal that cutting quality reduces significantly for composite structures. In this case, globules like resolidified material are formed at the rear side of the composite workpiece. The sideways burning of Kevlar laminate and resin is evident in composite structure cutting, which could be attributed to the oxygen being tapped during the manufacturing of the Kevlar laminate. Char formation on the surface of Kevlar laminate next to resin is observed. This would lower the bond quality between Kevlar laminate and mild steel sheet resulting in peeling off Kevlar laminate from the cut section. Consequently, cutting of mild steel and Kevlar laminate separately and joining them with resin forming a composite structure is better in terms of end product quality than laser cutting of composite structure as a whole.

Acknowledgments

The authors acknowledge the support of King Fahd University of Petroleum and Minerals Dhahran Saudi Arabia due to analytical tools for material characterization, and Karmetal due to laser cutting process.

References

1. A. Ivarson, J. Powell, J. Kamalu, and C. Magnusson, Oxidation Dynamics of Laser Cutting of Mild Steel and the Generation of Striations on the Cut Edge, *J. Mater. Process. Technol.*, 1994, **40**(3-4), p 359–374
2. P.S. Sheng and V.S. Joshi, Analysis of Heat-affected Zone Formation for Laser Cutting of Stainless Steel, *J. Mater. Process. Technol.*, 1995, **53**, p 879–892
3. J. Grum and D. Zuljan, Analysis of Heat Effects in Laser Cutting of Steels, *J. Mater. Eng. Perform.*, 1996, **5**(4), p 526–537
4. S. Roy and M.F. Modest, CW Laser Machining of Hard Ceramics – I : Effects of Three-dimensional Conduction, Variable Properties and Various Laser Parameters, *Int. J. Heat Mass Transfer*, 1993, **36**(14), p 3515–3528
5. B.S. Yilbas, J. Nickel, and A. Coban, Effects of Oxygen in Laser Cutting Process, *Mater. Manuf. Process.*, 1997, **12**(6), p 1163–1175
6. W. Schulz, D. Becker, J. Franke, R. Kemmerling, and G. Herziger, Heat Conduction Losses in Laser Cutting of Metals, *J. Phys. D: Appl. Phys.*, 1996, **26**, p 1357–1363
7. F. Quintero, F. Varas, J. Pou, Lusquinos, and M. Boutinguiza, Theoretical Analysis of Material Removal Mechanisms in Pulsed Laser Fusion Cutting of Ceramics, *J. Phys. D: Appl. Phys.*, 2005, **38**, p 655–666
8. D.K. Shanmugam, F.L. Chen, E. Siores, and M. Brandt, Comparative Study of Jetting Machining Technologies Over Laser Machining Technology for Cutting Composite Materials, *Compos. Struct.*, 2002, **57**, p 289–296
9. A.A. Cenna and P. Mathew, Evaluation of Cut Quality of Fibre-Reinforced Plastics – A Review, *Int. J. Machine Tools Manuf.*, 1997, **37**(6), p 723–736
10. C.C. Chen and W. Cheng, Material Properties and Laser Cutting of Composites, *Int. SAMPE Tech. Conf.*, 1991, **23**, p 274–287
11. L.M. Galantucci and F. Giusti, Excimer Laser Cutting: Experimental Characterization and 3D Numerical Modeling for Polyester Resins, *CIRP Ann. – Manuf. Technol.*, 1998, **47**(1), p 141–144
12. V. Tagliaferri, A. Dillio, and V.I. Crivelli, Laser Cutting of Fibre-Reinforced Polyesters, *Composites*, 1985, **16**(4), p 317–325
13. D.J. Doyle and J.M. Kokosa, Laser Cutting of Kevlar. A Study of the Chemical By-Products, *Mater. Manuf. Process.*, 1990, **5**(4), p 609–615
14. A. Kar, J.A. Rothenflue, and W.P. Latham, Scaling Laws for Thick-Section Cutting with a Chemical Oxygen-Iodine Laser, *J. Laser Appl.*, 1997, **9**(6), p 279–286
15. D. Schuocker, The Physical Mechanism and Theory of Laser Cutting, in *The Industrial Laser Annual Hand Book*, D. Belforte and M. Levitt, eds. Penn Well Books, Tulsa, 1987, pp. 65–79
16. J.O. Hirschfelder, C.F. Curtiss, and R.B. Bird, *Molecular Theory of Gasses and Liquids*. John Wiley & Sons, New York, 1954, p 14